3D Computational Simulation and Experimental Validation of Structured Materials: Case Studies of Tissue Papers

Flávia P. Morais,[a,*] and Joana M. R. Curto [a,b]

The development and optimization of structured materials, such as tissue paper materials, benefit from modeling strategies that take into consideration its structural hierarchy at the fiber and the paper levels. The use of an innovative three-dimensional voxel approach to model both the fiber and the 3D paper structure were validated by comparison of the computational structures with the laboratory-made structures. The main goal of this work was to model tissue structures and obtain a computational implementation adapted for tissue products. The fibers were modeled in 3D according to their dimensions, and the structures produced by them were characterized using the Representative Elementary Volume (REV) and image analysis computational tools. This methodology made it possible to model the fibers according to their morphology, flexibility, and collapse, resulting in a tissue structure with thickness, porosity, relative bonding area, coverage, among other properties. The experimental design plan included the production and characterization of isotropic laboratory structures with basis weights of 20, 40, and 60 g/m^2 with different eucalyptus fibers and beating degrees. With the aid of these advanced computational tools, mathematic models with predictive capacity for tissue properties such as softness, strength, and absorption can be developed.

DOI: 10.15376/biores.17.3.4206-4225

Keywords: 3D Fiber models; Eucalyptus pulp fibers; Representative elementary volume (REV); Structural properties; Tissue paper materials; Validation

*Contact information: a: Fiber Materials and Environmental Technologies (FibEnTech-UBI), Universidade da Beira Interior, R. Marquês de D'Ávila e Bolama, 6201-001 Covilhã, Portugal; b: Chemical Process Engineering and Forest Products Research Centre (CIEPQPF), Universidade de Coimbra, R. Sílvio Lima, Polo II, 3004-531 Coimbra, Portugal; *Corresponding author: flavia.morais@ubi.pt*

INTRODUCTION

Fibrous paper materials, such as tissue products, for their multiplicity, cost-effectiveness, cleanliness, and convenience, play an important role in society. The study and validation of computational methods to optimize these materials play an important role in the ability to improve them. Our approach combines an experimental and computational plan design for the development of three-dimensional (3D) paper networks models able to correlate the influence of 3D fiber dimensions and properties and the structures formed by them (Conceição *et al.* 2010; Curto *et al.* 2011) and to optimize these types of materials (Lavrykov *et al.* 2012; Morais *et al.* 2020a,b). 3D paper images are also used to create databases of microstructural descriptors for a complex fiber network (Marulier *et al.* 2015), and model their properties, combining a realistic configuration of cellulosic fibers by macroscale methods (Kettil *et al.* 2018).

Paper materials' multi-scale structural characterization constitutes an ongoing challenge that could be accessed using a combination of different analysis methods (Chinga-Carrasco 2009). Due to the complexity and non-uniformity of these materials, their quantification may be difficult. To investigate the properties and structures of different tissue paper materials, numerical simulations of material features are needed (Wiltsche *et al.* 2011; Sun *et al.* 2021). Several methods are used to characterize pores at nano, micro, and macroscale (Lawrence and Jiang 2017; Morais *et al.* 2021a). Image analysis methods using computational tools are effective in pore properties characterization in processed images from SEM, for example (Chinga-Carrasco and Helle 2002; Raunio and Ritala 2013). To use an image fraction for this type of analysis, the image fraction must be representative of the original image. This fraction must represent the material for a respective property and be wide enough to contain satisfactory information about the porous structure to be statistically representative (Bloch and Roscoat 2009). It is necessary to prove that the representative elementary area (REA) or volume (REV) is satisfactory to allow the quantification of porosity and pore size and distribution (Kanit *et al.* 2003; Bloch and Roscoat 2009; Dirrenberger *et al.* 2014).

Tissue paper materials are optimized according to their intended use, including toilet papers, paper towels, napkins, facial papers, tissue masks, among others. The key properties to evaluate tissue product performance are bulk, porosity, softness, strength, and absorption (Raunio and Ritala 2012; de Assis *et al.* 2018; Morais *et al.* 2019, 2021b). These properties depend especially on the fiber properties (Fig. 1), especially the fiber transverse dimensions (fiber wall and lumen), and densification (fiber flexibility and collapsibility) (Paavilainen 1993a,b). In addition to these fiber characteristics, tissue properties are also affected by fiber chemistry, fiber orientation, papermaking chemistry, and technologies used to produce these materials, among other aspects; however, the present work is focused on the fiber morphological/physical properties, as well as the paper structural properties.

Establishing relationships between fiber properties and the structures formed by them, based on experimental data, is very complex due to the variability of fiber dimensions in each raw material used in its production. Furthermore, fiber flexibility and collapse are two mechanisms that occur simultaneously when studying the densification of paper structures (Bloch *et al.* 2019). For this reason, 3D paper modeling has been considered a useful computational tool to overcome these experimental limitations. To the best of our knowledge, there has been a deficiency of research to relate the 3D fiber dimensions with low basis weight and high porosity structures, such as tissue materials, with the aim not only to improve their properties but also to model these structures with 3D fiber-based simulators. However, 3D fiber-based simulation studies arise for other low-density fibrous materials such as nonwovens.

Nonwoven are materials applied to surgical, cosmetic masks, *etc*., produced by the random deposition of short (staple fibers) or infinitely long fibers (continuous filaments) on top of each other, bonding them by mechanical, thermal, or chemical processes (Pourdeyhimi *et al.* 2006). Numerical models used allowed the modeling and simulation of the 3D geometry of fiber webs, to optimize the performance of these materials at a laboratory and industrial level (Pourdeyhimi *et al.* 2006; Grothaus *et al.* 2014; Jirsák *et al.* 2022; Xie *et al.* 2022). This motivated us to design an innovative methodology for model tissue structures and predict the structural and functional properties, optimizing the various tissue materials (Morais *et al.* 2020a,b).

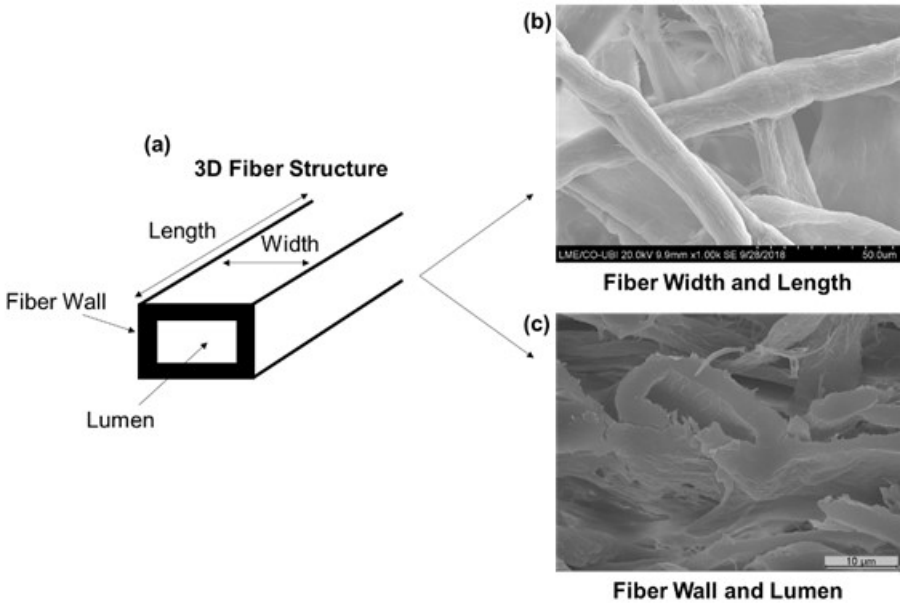

Fig. 1. Illustration of the (a) fiber morphology. Scanning electron microscopy (SEM) images of (b) fiber length and fiber width and (c) fiber wall and lumen. These are images of isotropic laboratory paper structures obtained using SEM.

Over the years, material modeling has become an important tool in the development and design of materials with better performance. The computational tools make it possible to significantly reduce the experimental work in the new materials development, to have a better synergy between the experimental tests design, and to carry out the simulation of materials specific properties (Niskanen *et al.* 1997; Dodson *et al.* 2001, 2002; Alava and Niskanen 2006; Sampson 2009). An approach to modeling the relationships between the key parameters and the functional properties of tissue materials is essential for the advances achieved in the field of fibrous materials science, engineering, and modeling. The authors' previous work involved the design of 3D fiber models for each fiber population from different types of raw materials, in order to simulate and optimize tissue papers (Morais *et al.* 2020a,b). The tissue structure modeling is achieved using a fibrous material simulator, implemented and validated by Conceição *et al.* (2009) and Curto *et al.* (2011), designated by *voxelfiber*. This simulator was previously validated for printing and writing paper (Curto 2012); however, it was not validated and applied to low basis weight and high porosity materials. The structures are simulated and compared with the real structures. *Voxelfiber* is based on a cellular automata, in which there is a Cartesian division of cells so that each fiber is represented as a sequence of voxels, each occupying a pre-established volume (Conceição *et al.* 2009; Curto *et al.* 2011). The fibers are also deposited one by one, each fiber occupying its space. Depending on its position, dimension, and flexibility, the fiber obeys the underlying structure (Fig. 2a,b,c). This fiber model includes the fiber internal structure and the possibility to change it and have collapsibility in the material Z-direction (Curto *et al.* 2011; Morais *et al.* 2020b). This innovative 3D voxel approach considers the modeling at the fiber level and the paper structure level. The *voxelfiber* can also be extended to incorporate other fiber sedimentation possibilities and for other fibrous materials, such as micro/nanocellulose-derived products (Curto 2012; Martins *et al.* 2018; Morais *et al.* 2020c).

To achieve these goals, it is necessary to introduce 3D fiber data to obtain a computational implementation adapted for tissue products, as well as to validate structures developed in the 3D computational simulator by comparison with structures produced in the laboratory. This simulation approach can also be applied to real tissue papers by adjusting the simulator by introducing the physical processes used in these materials such as fiber orientation, creping, and embossing processes (Raunio and Ritala 2012; Raunio *et al.* 2018). These advanced computational tools developed with predictive capacity can determine the most promising raw materials for a specified tissue paper and which process operations are needed to obtain a material with optimized properties. The novelty of this work is to demonstrate an experimental and computational approach to 3D fiber characterization and modeling to forecast tissue characteristics, optimizing the performance of tissue materials. Figure 2 presents an outline of this work. The first part of this work presented 3D fiber and structure characterization, and the second part demonstrated a 3D modeling approach to include key fiber and structure parameters and simulate a concrete fibrous material. For this purpose, the computational model was applied to eucalyptus-based tissue papers. As these types of products are mainly produced from eucalyptus pulps, it is important to assess the contribution of this raw material with different biometry and morphology to the final properties. Therefore, two different eucalyptus pulps were subject to a refining treatment to implement the behavior in the Z-direction (thickness) and different flexibilities and fiber collapse degrees into the model. Additionally, these computational studies were validated by comparing laboratory-made structures with different basis weights. The measured properties, such as the thickness and porosity, were compared with the estimated properties. Therefore, the influence of fiber and structure properties was evaluated and investigated to study and predict the properties of tissue paper materials.

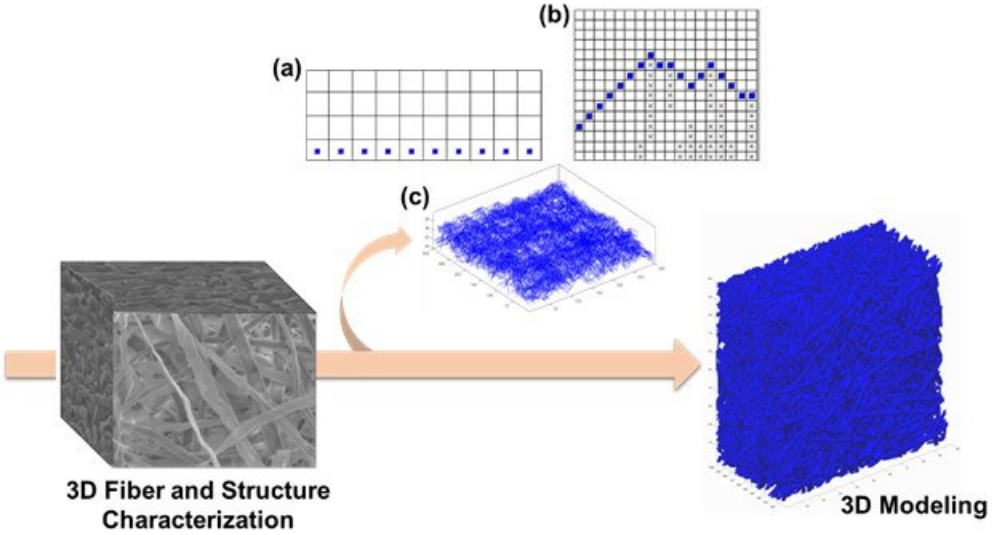

Fig. 2. Outline of the different steps for the development of this work. The first part includes a 3D fiber and structure characterization, and the second part presents a 3D modeling approach. To achieve these computational simulation studies, fibers are modeled with realistic parameters based on experimental analysis. The 3D computational structure is produced with the random deposition of fibers, (a) one by one, (b) not depositing on others since the space occupied by the fibers will not be overlaid, (c) under a spatial organization in the 3D matrix.

EXPERIMENTAL

Materials

Two industrial bleached eucalyptus kraft pulps were used in this work after disintegration according to ISO 5263-1. These samples differed in the bleaching steps (ECF – Elemental Chlorine Free and TCF – Total Chlorine Free) and one was air-dried (EUC) and the other was never-dried (EUC Slush). Both pulps were selected as they are representative eucalyptus pulps in a tissue paper manufacture.

Methods

An experimental design was conceived to characterize the samples to quantify the fiber influence and beating degree, allowing the implementation of different flexibility and fiber collapse degrees into the computational studies. The pulps were beaten in a PFI mill at 500, 1000, and 1500 revolutions under a refining intensity of 3.33 N/mm, according to ISO 5264-2. A methodology to produce the laboratory-made isotropic structures with different basis weights and with pressing step suppression was proposed following an adaptation of ISO 5269-1, to mimic tissue papers and evaluate their properties. The samples were also conditioned at 23 ± 1 °C, with a relative humidity of 50 ± 2%, according to ISO 187. Although some functional properties would vary depending on the fiber orientation in the structures (anisotropy phenomenon), it should be noted that in this work, only isotropic structures were considered in order to follow a standardized method. Additionally, the simulator used in the studies, *voxelfiber*, was developed and implemented to simulate the random deposition of fibers, as isotropic laboratory structures are produced. Therefore, computational simulation of 3D fiber networks is more realistic and comparable to real structures.

The morphological properties of modified pulp fibers were determined automatically by image analysis of a diluted suspension (20 mg/L) in a flow chamber in the fiber analyzer MorFi (TECHPAP, Grenoble, France). This data included the fiber length weighted by length, fiber width, coarseness, and fines content. The fibers are defined by lengths between 200 μm and 10 mm, and widths between 5 and 75 μm. The fine elements present lengths less than 200 μm and widths less than 15 μm. The fiber coarseness is measured according to the ratio of the mass of all fibers to the total length, considering the number of processed images, the imaged volume, and the pulp fiber consistency (Tourtollet *et al.* 2003). The assays were performed in triplicate, and the values presented are the mean and standard deviation of these three measurements.

The pulp suspension drainability was evaluated, in triplicate, by the Schopper–Riegler degree method, according to ISO 5267-1.

Scanning electron microscopy (SEM) was used to characterize the 3D network surface (XY direction) and cross-sections (Z-direction) of handsheets. The samples were gold plated using a Sputter Quorum Q 15 OR ES equipment (Laughton, East Sussex, UK), and analyzed by Hitachi S2700 SEM (Tokyo, Japan), with a Bruker detector (Karlsruhe, Germany) operating at +20 kV and different magnifications. In the cross-section of the handsheets, the effective thickness of each fiber (cell wall fiber + lumen fiber) was measured, according to the method described by Morais *et al.* (2020a). The vector placement method was used to measure about 300 to 400 different fibers, along the entire handsheet cross-section. To ensure that each fiber was measured only once, without duplication, all fibers were identified, numbered, and measured. Additionally, SEM images were processed and analyzed using image analysis software, the *ImageJ*, for surface pore

size distribution characterization, with defined criteria for the stabilization of the average of measured values (Hotaling *et al.* 2015). An image fraction of the 3D network was selected to contain an elementary area representative of the structure's pores. This area represented the overall structure for pore properties and contained satisfactory 3D network information to be statistically representative (Hotaling *et al.* 2015; Morais *et al.* 2020b). Binary images were segmented, processed, and analyzed, generating summary statistics for pore properties. Additionally, several morphological processing algorithms were used to process these binary images, including correcting the shadow gradient, reducing noise, obtaining an image detail, improving edges, creating higher contrast between light and dark areas, and removing isolated fibers (Morais *et al.* 2021a). A systematic method was used to generate pore dimension and distribution statistics. About 500 to 1500 pores were measured from at least three SEM images per sample. This analysis was carried out for the different samples presented in this work; however, as a proof of concept, in the results and discussion section, only the results for the samples without beating, with a basis weight of 20 g/m^2 are presented.

The structural properties of the handsheets, such as basis weight, thickness, using a micrometer (FRANK-PTI GMBH, Birkenau, Germany), and bulk, were determined according to ISO 12625-3 and ISO 12525-3. The handsheet apparent porosity (%) was also calculated theoretically as shown in Eq. 1 (Morais *et al.* 2020b, 2021a).

$$\text{Porosity} = 1 - (\text{density of the handsheet} / \text{density of cellulose, } 1.5 \text{ g/cm}^3) \quad (1)$$

COMPUTATIONAL STUDIES

A 3D simulator (https://github.com/eduardotrincaoconceicao/voxelfiber) of fibrous materials, the *voxelfiber*, was used to simulate the 3D structures with the fiber dimensions obtained experimentally. A more detailed description of the 3D simulator can be found in Conceição *et al.* (2009) and Curto *et al.* (2011). This simulator allows the modeling of porous structures as planar random networks (Fig. 2). The 3D simulator uses fiber dimensions and properties as input parameters and produces the resulting 3D structure made from these fibers. The input parameters are length/width ratio, fiber wall thickness, lumen thickness, fiber flexibility, and resolution (number of layers in the thickness direction, up to 0.05 μm). Curto (2012) established relationships between fibers and structural properties of paper based-materials, developing and validating this 3D model. In Curto's studies, the fiber flexibility was determined experimentally, in which the values determined corresponded to the extreme values of different fibers. Therefore, that study constituted valuable information in order to be applied to other fibers with fiber dimensions and properties in the same range. In the present work, the fiber flexibility was estimated according to these works developed previously simultaneously with a methodology of SEM image analysis, described above, to be inputted in the model. The 3D computational structures will be processed to obtain important properties, such as thickness (local and average), porosity (interfiber and global), relative bonded area (RBA), coverage, number of crossings per fiber, among others (Morais *et al.* 2020a,b). RBA corresponds to the fraction of fiber surface in contact with other fibers and is described as the ratio between the fibers' bonded area and the total surface area of the fibers. Coverage is the number of fibers covering a given point on the surface of the paper material. In the present work, average thickness, interfiber porosity, RBA, and coverage were evaluated to determine the

REV, and the estimated properties of average thickness and global porosity were compared to the same experimental measured properties. The adjustments of uniform model parameters were performed, so that it reproduces realistic results, according to experimental datasets independent of the laboratory-made structures. Under conditions other than calibrated, the computational model was verified, examining its ability to realistically represent the desired properties. Computational studies were performed using Matlab® (R 2020a, 9.8.0.1323502, MathWorks, Natick, MA, USA).

RESULTS AND DISCUSSION

Pulp Fiber and Structure Experimental Characterization

Eucalyptus fibers present high homogeneity as well as other characteristics such as high fiber wall thickness, resistance to collapse, fibrous population, low fines content, among others when compared with other fibers used in tissue products, which results in good drainage, formation, runnability, high bulk, absorption, and softness (de Assis *et al.* 2018). The two investigated raw materials with different beating degrees presented different fiber morphology (Table 1). The changes were more visible in the EUC Slush sample, since this pulp was a more degraded pulp with lower drainability (25°SR), more deformations, and fibrillation as a result of its bleaching sequence (TCF), compared to the EUC sample. In the hornification process during the drying of the EUC sample, a fraction of the pores in the cell wall collapsed and closed irreversibly due to the formation of hydrogen bonds between adjacent surfaces, leading to fibril aggregation or coalescence (Giacomozzi and Joutsimo 2015). It would be expected that this sample presented high deformations (Giacomozzi and Joutsimo 2017). However, the oxygen and ozone bleaching stage process promote a more intense degradation of polysaccharides and consequent loss of yield and pulp properties, such as decreased intrinsic viscosity and high fine content (Masrol *et al.* 2017; Morais *et al.* 2021a).

Table 1. Fiber Morphology and Pulp Drainability of EUC and EUC Slush Samples

Fiber Types	PFI refining revolutions	FL* (mm)	FW* (µm)	C* (mg/100m)	FC* (%)	ºSR
EUC	0	0.798 ± 0.004	19.1 ± 0.1	6.83 ± 0.11	37.1 ± 0.3	20 ± 0
	500	0.770 ± 0.002	19.3 ± 0.1	6.86 ± 0.10	40.7 ± 0.9	23 ± 0
	1000	0.764 ± 0.002	19.5 ± 0.1	6.67 ± 0.07	41.5 ± 0.2	27 ± 0
	1500	0.757 ± 0.002	19.6 ± 0.1	6.77 ± 0.07	42.3 ± 0.6	32 ± 0
EUC Slush	0	0.729 ± 0.003	19.1 ± 0.0	6.31 ± 0.04	38.5 ± 0.4	25 ± 0
	500	0.701 ± 0.002	20.2 ± 0.2	6.62 ± 0.10	45.7 ± 0.6	32 ± 0
	1000	0.683 ± 0.002	20.6 ± 0.2	6.84 ± 0.07	46.8 ± 0.9	47 ± 0
	1500	0.665 ± 0.003	20.7 ± 0.2	7.06 ± 0.07	50.4 ± 0.9	70 ± 0

* FL: fiber length weighted by length; FW: fiber width; C: coarseness; FC: fines content; ºSR: Schopper–Riegler degree

The fiber length weight by length (FL) decreased over the PFI revolutions, contrary to the fiber width (FW), coarseness (C), and fines content (FC). Fiber fibrillation after beating decreases coarseness; however, the coarseness increase can be explained by the decrease in fiber length, since is described as the mass per length unit. These results can be

explained by the presence of some fine elements that were not accounted for in the measurements. This evidence reduces the fiber length and, consequently, increases fine content, despite the high fiber coarseness (Joutsimo and Asikainen 2013; Morais *et al.* 2021a). The beating process increased the fines content corresponding to a higher degradation of the cellulosic chains (degraded and less rigid fibers), and consequently to a loss of the fiber intrinsic strength (Muneri 1997; Morais *et al.* 2021a). The effect of mechanical refining enhanced efficient fibrillation, which negatively affected the drainability, as verified by the ºSR values increase (Table 1). This property is influenced by fiber external fibrillation and the amount of fine elements and related with the fibers' flexibility and the improvement of their bonding capacity. This effect was especially noticeable for the EUC Slush sample, where a maximum increase of 180% can be observed, while for EUC sample a maximum increase of 60% can be observed. Dry EUC fibers can become more conformable when refined, producing fines and, consequently, increasing drainage resistance, requiring considerable energy expenditure. Furthermore, the changes caused by drying are not fully reversible (Seth 2001). Considering also that both pulps have different bleaching stages, the never-dried fibers of EUC Slush were fibrillated to a much higher extent than the dry fibers of EUC, increasing the fines content and consequently the ºSR values. Light refining between 22 and 35 ºSR is recommended for eucalyptus pulps to produce high-quality tissue papers (de Assis *et al.* 2018). Therefore, it is considered that the EUC pulp must be refined up to 1500 revolutions and the EUC Slush pulp must be refined up to 500 revolutions.

Suspended fibers are not subjected to the tensions found in the handsheets, so the fiber morphology may be different when fibers are in water suspension or the paper structure. SEM is a method that provides information about the fibers in the paper structure. The fiber dimensions and the collapse degree can be measured and estimated in the handsheet cross-section, using this methodology. Kallmes and Bernier (1963) stated that the best representation of the effective fiber thickness cross-section is a rectangle to accurately determine measurements of this 3D fiber dimension, which includes the fiber wall and lumen, in the paper structure. They also stated that in the handsheets formation, pressures are applied to the fibers causing fiber collapse, with considerable variations in cross-sectional thickness (Kallmes and Bernier 1963). In previous work, the authors analyzed the effective fiber thickness, the third fiber dimension of eucalyptus pulp fibers without beating, through the vector placement method on a significant number of fibers in the handsheet cross-section (Morais *et al.* 2020a). The experimental results for effective fiber thickness distribution were obtained using this approach (Fig. 3). The effective fiber thickness of EUC and EUC Slush samples presented values, on average, of 3.92 ± 1.57 µm and 4.77 ± 1.23 µm, respectively. This suggests that EUC Slush fibers present a thicker cell wall compared to EUC fibers. This evidence can also be explained by fiber length weighted by length and coarseness (Table 1). The effective fiber thickness (fiber wall plus lumen) data are essential to predict the handsheets properties of eucalyptus pulp fibers, such as thickness, bulk, and porosity (Pulkkinen *et al.* 2006). By following these fiber modifications in the 3D structure, together with the coarseness properties, a realistic approach of the dimensions in the paper Z direction can be performed, to accurately model the fibers in simulators based on 3D modeling of these structural elements (Morais *et al.* 2020b).

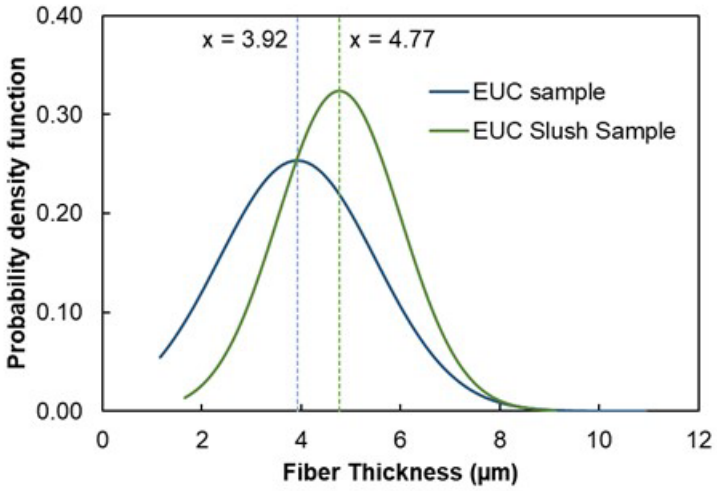

Fig. 3. Fiber effective thickness normal distribution of EUC and EUC Slush samples, in comparison to the arithmetic mean (vertical line)

This approach of measuring the effective fiber thickness in paper structure is only possible to be carried out in structures without refining operation since the densification that occurs from changing the fiber flexibility and collapse with beating is evident. Figure 4 showed an example of this densification effect on the handsheet cross-section of EUC Slush sample with zero and 1500 revolutions.

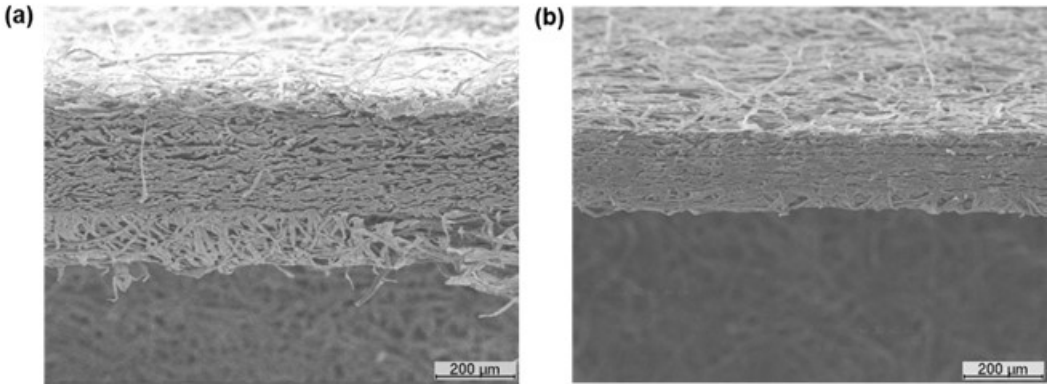

Fig. 4. SEM images of EUC Slush sample handsheet cross-section, with (a) zero PFI revolutions (basis weight of 60 g/m^2 with a thickness of 249 µm) and (b) 1500 PFI revolutions (basis weight of 60 g/m^2 with a thickness of 138 µm) (magnification: 100x)

Additionally, Fig. 5 presents the SEM images of the EUC and EUC Slush samples without beating, as well as the pore size distribution in the 3D network surface handsheets. These multi-structured materials presented a 3D network of non-oriented cellulosic fibers and an irregular porous structure. The optimization of these structures is essential to produce optimized tissue papers with improved functional properties, such as softness, strength, and absorption. The porous structure and the pore surfaces of these types of materials are essential for absorption properties, especially by paper towels. Also, the pores allow the penetration of additive agents, such as softeners or lotions that are sprayed on the sheet surface, providing space for their deposition, improving the final strength and softness properties of toilet papers and napkins, for example (Rowland 1977; Neumann *et*

al. 2016). This ability of additives to migrate through the material depends on the irregular pore distribution, pore size that varies over a wide range, and the tortuous paths that the pores provide for the flow of the liquids (Neumann *et al.* 2016). The EUC and EUC Slush samples showed average pore sizes of 14.20 ± 13.02 µm and 12.98 ± 8.05 µm, respectively. The characteristics of the EUC Slush sample, such as TCF bleaching stage, lower fiber length, and higher fine content and ºSR, benefited the inter-fiber bonding, filling in the empty spaces between fibers and, consequently, reducing the pore dimension and distribution in the structures (Morais *et al.* 2021a). These features correspond mainly to the handsheet surface and do not necessarily extrapolate the handsheet bulk. This analysis demonstrated the heterogeneity of 3D networks from the high standard deviation due to the presence of numerous deep pores in contrast to the larger pores on the surface. In addition, the global porosity, across the sheet thickness, was calculated, and the results are shown in Fig. 6. These computational image analysis tools can also analyze the pore properties of computationally simulated structures. An analysis of the pore dimension and distribution can be performed in the 3D computational structure network and compared with the experimental structure.

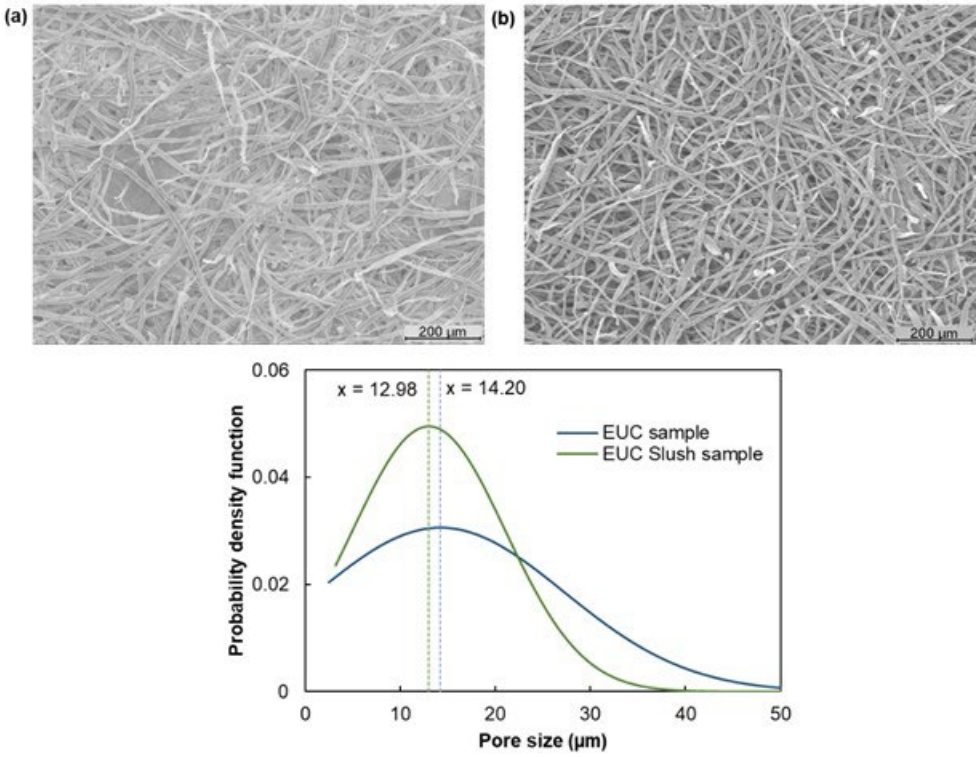

Fig. 5. SEM images of (a) EUC and (b) EUC Slush samples (magnification: 100x), and pore size distribution in the 3D network surface handsheets

Tissue papers have structural characteristics of low basis weight paper materials. In the production of these types of materials, different individual sheets are used. Therefore, the basis weight and thickness properties of tissue papers directly depend on the number of sheets in their composition. For this reason, three different basis weights were investigated to mimic these individual sheets in tissue papers. A structure with 20 g/m^2 can correspond to a tissue base industrial sheet, a structure with 40 g/m^2 can correspond to a product made up of 2-ply sheets of 20 g/m^2, and a structure with 60 g/m^2 can correspond

to a product made up of 3-ply sheets of 20 g/m^2 or even 2-ply sheets of 30 g/m^2. It should also be noted that in this work the creping stage was not considered, in order to separate the effects of this operation, as it constituted a multifactorial challenge (multiple-input multiple-output (MIMO) approach), mainly due to relationships between pulp fibers, the multiple changes resulting from the different processes, and the functional tissue properties (Morais *et al.* 2021c).

The evolution of structural properties against PFI revolutions for EUC and EUC Slush handsheets with different basis weights are presented in Fig. 6. The pulp fibers were beaten in four beating levels (0, 500, 1000, and 1500 PFI revolutions). As to be expected, the results indicate that the handsheets thickness increased with the basis weights and decreased with the PFI revolutions. Inversely, the bulk and porosity decreased with the basis weights and PFI revolutions. This evidence is explained by the definitions of basis weight (weight per unit area), thickness, bulk, and porosity. For a given basis weight, thickness determines how bulky or dense paper is, since a structure produced with a refined pulp presents lower thickness. Bulk, reciprocal of density, indicates the volume or thickness in relation to weight, and it is calculated from thickness and basis weight. Porosity is the volume fraction not occupied by the fibers within a paper sheet, and it is simply obtained by dividing the volume of all the voids by the total volume of the sheet. Considering these definitions, structures with higher basis weight are thicker, denser, and, consequently, less porous. Additionally, the differences found in these structural properties are due to the different eucalyptus pulps, with different production processes, used to produce the handsheets.

Fiber flexibility changes during the beating. The possibility of modeling this parameter is very important for the model performance evaluation. When comparing these two eucalyptus pulps, the information about fiber flexibility and biometry is determinant to predict structural properties. The extreme values of fiber wall thickness, beating ability, and flexibility correspond to the different eucalyptus used in tissue paper manufacture. Fiber flexibility and conformability are related to the structure density and porosity, and consequently to the fiber morphology and the modulus of the cell wall, which also present an effect on fiber bonding (Paavilainen 1993a). EUC Slush presented higher values of effective fiber thickness (Fig. 3) and consequently, it was less flexible (Fig. 6) than the thinner fibers of EUC sample. This provides EUC Slush fibers with higher resistance to collapse and individual fiber stiffness than EUC fibers, to produce bulky structures with loosely bonded fibers (higher porosity). These experimental results for the evolutions of structural properties, together with fiber thickness and flexibility, constitute valuable information, also applicable for other eucalyptus fiber pulps, with fiber dimensions in this range. After this quantification, the key property of flexibility is included in the structural model, with fiber bending in the Z-direction as an important parameter. The implementation presents full discretization of space in both the in-plane and out-of-plane directions, and an approach using cellular automata to drive fiber bending (Curto 2012).

Depending on the specific use of each tissue product, the control of the bulk and porosity, which are thickness' dependent, may be particularly relevant. For tissue papers, a high bulk is required to ensure the development of the final end-use properties (Morais *et al.* 2019). The experimental study of paper structures with different basis weights also provides important data for 3D paper model calibration and validation processes to obtain a paper simulator with a predictive capacity.

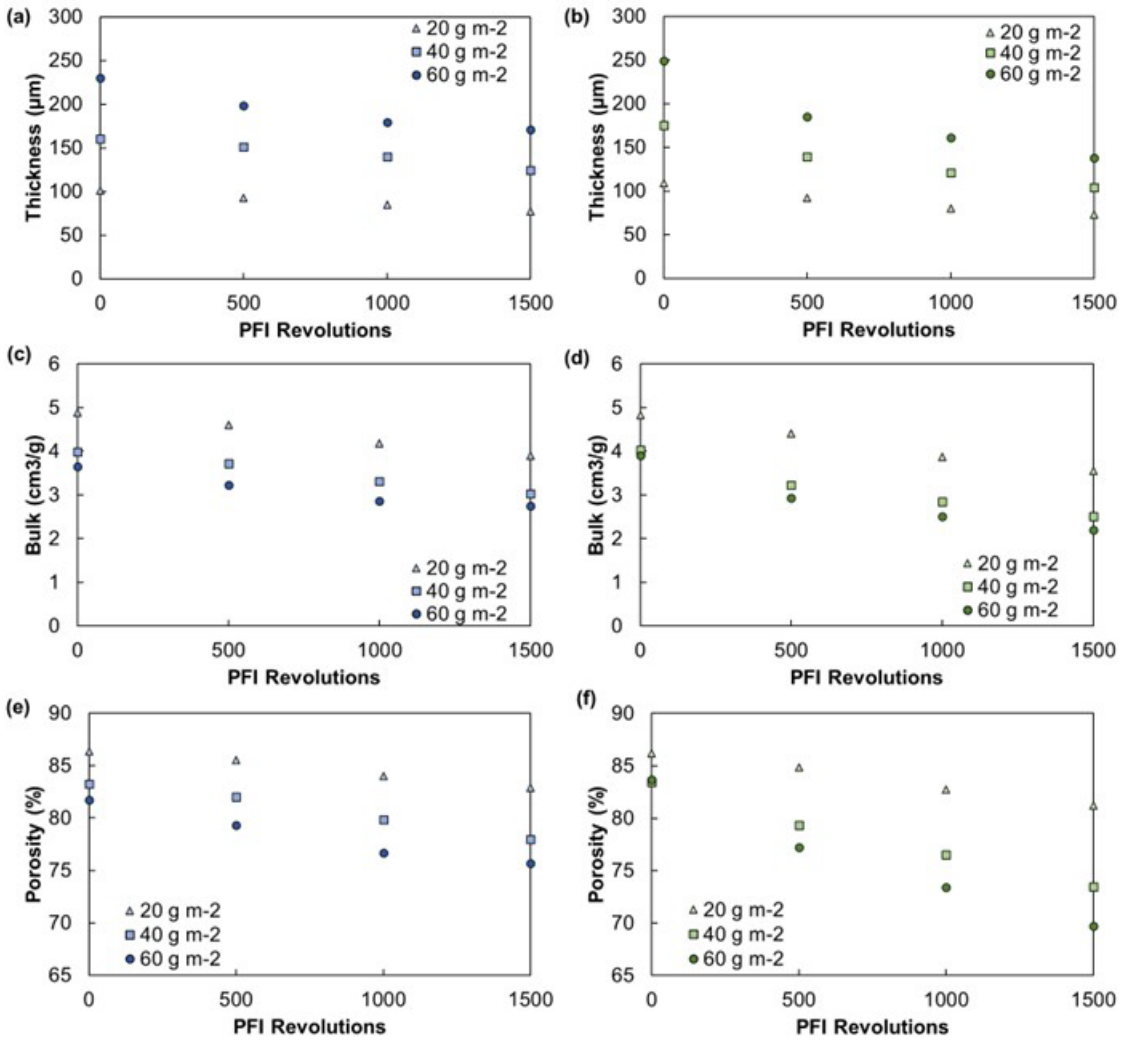

Fig. 6. Structural properties, such as (a, b) thickness, (c, d) bulk, and (e, f) porosity as a function of PFI revolutions of (a, c, e) EUC and (b, d, f) EUC Slush handsheets with 20, 40, and 60 g/m^2

Computational Simulations and Representative Elementary Volume (REV)

The structures produced with different basis weights and beating degrees can be simulated computationally to optimized tissue paper materials. Beating presents a major effect on the fiber flexibility, and consequently on its collapse in the paper structure. Figure 7 shows an example of the computational simulations that can be obtained for the EUC sample. The computational simulation model was used to perform simulation studies. In these case studies, it was used to investigate the relative influence of fiber flexibility, dimensions, and collapsibility. The model includes these key fiber properties as well as process operations such as fiber deposition, network formation, and densification. Therefore, simulation studies allow one to separate the influence of these papermaking fiber properties on the structure densification, for example, which occurs with beating.

The multiscale model gave realistic predictions and enabled us to link fiber microstructure and structural properties. The computational model simulates a structure similar to the real one obtained experimentally, with a distinction between the XY plane (Fig. 7a, b) and the Z plane (Fig. 7c, d). The fibers' properties and dimensions obtained by the fiber analyzer, MorFi, as well as the data of fiber morphology and behavior in the z-

direction, obtained by the vector placement method in SEM images, are considered to promote a more realistic computational representation (Morais *et al.* 2020a).

The uniform model parameters were adjusted to reproduce realistic results according to experimental datasets independent of the laboratory-made structures (Morais *et al.* 2020a). Under conditions other than calibrated, the computational model was verified, examining its ability to realistically represent the properties. To increase the reliability of the computational model, an independent set of the initial structures produced was used to validate the 3D computational model. The fibers were randomly positioned and oriented in the XY plane to simulate the formation of isotropic laboratory handsheets (the ones used to validate the model). The model output is a 3D fiber network structure formed with occupied and empty voxels, in which the information concerning each fiber is kept. At this stage, this formed structure can predict several structural properties such as thickness (local and average), porosity (interfiber and global), RBA, coverage, and the number of crossings per fiber.

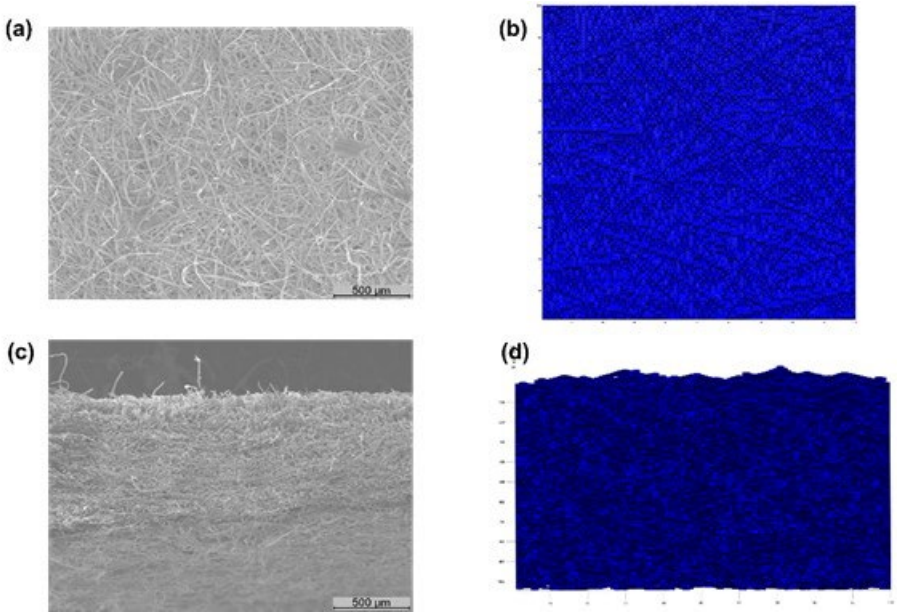

Fig. 7. SEM images of the experimental structure of the EUC sample with a basis weight of 40 g/m^2 in the XY plane (a) and Z plane (c), and the respective computational images in the XY plane (b) and Z plane (d), using the 3D computational simulator descript in (Conceição *et al.* 2010; Curto *et al.* 2011; Morais *et al.* 2020b)

The fibers are modeled and simulated three-dimensionally by their random deposition, representing a good estimative of the real handsheets network. The model includes key fiber properties such as morphology, flexibility, and collapsibility, and process operations such as fiber deposition, network forming, or densification. Additionally, the model considers the fiber microstructure level, including lumen and fiber wall thickness, with a resolution up to 0.05 µm (Curto 2012). 3D computational simulations with this 3D data are essential to optimize the final end-use properties of tissue paper materials.

The REV is the key concept in determining and modeling the different properties of heterogeneous materials (Doškář *et al.* 2018; Hu *et al.* 2018). A REV should be large enough to accommodate sufficient properties information from the structures and, at the same time, small enough to comply with scales separation (du Roscoat *et al.* 2007;

Mirkhalaf *et al.* 2016). For this purpose, the REV was determined for different properties in the computational structure. A systematic analysis was performed of the influence on the thickness, interfiber porosity, RBA, and coverage of the XY plane (Fig. 8). The structures were formed by the random deposition of single fibers in this plane to simulate the formation of handsheets. The fibers were modeled according to their length/width ratio (38), fiber flexibility (1), wall thickness (2), lumen thickness (0), and the number of fibers (24500). The information in parentheses corresponds to the values used in the simulations to represent each parameter. The length/width ratio was obtained from the experimental data; fiber flexibility, wall thickness, and lumen are represented in computational voxel units; and the number of fibers was automatically defined by establishing the basis weight of the structures in the model. A fiber flexibility equal to one corresponds to a less flexible fiber, and a wall thickness equal to two and a lumen equal to zero corresponds to a fully collapsed fiber, with an effective fiber thickness of four voxels. The proposed fiber models based on an experimental analysis, with differences between fiber morphology and dimensions, collapse degrees, and flexibility, result in structures with different structural properties (Morais *et al.* 2020b). These input parameters were kept constant, and the dimensions of the XY plane (between 10 to 300) were changed through the simulations. According to Fig. 8, the structural properties become more stable and tend towards experimental values while XY plane dimensions increase. For a given XY plane dimension superior to 200, the structural properties reach a practically constant value. The results indicated that these properties depend on the size of the volume in the XY plane. Therefore, to carry out the different computational simulations, we decided to use an XY plane with dimensions of 300 × 300.

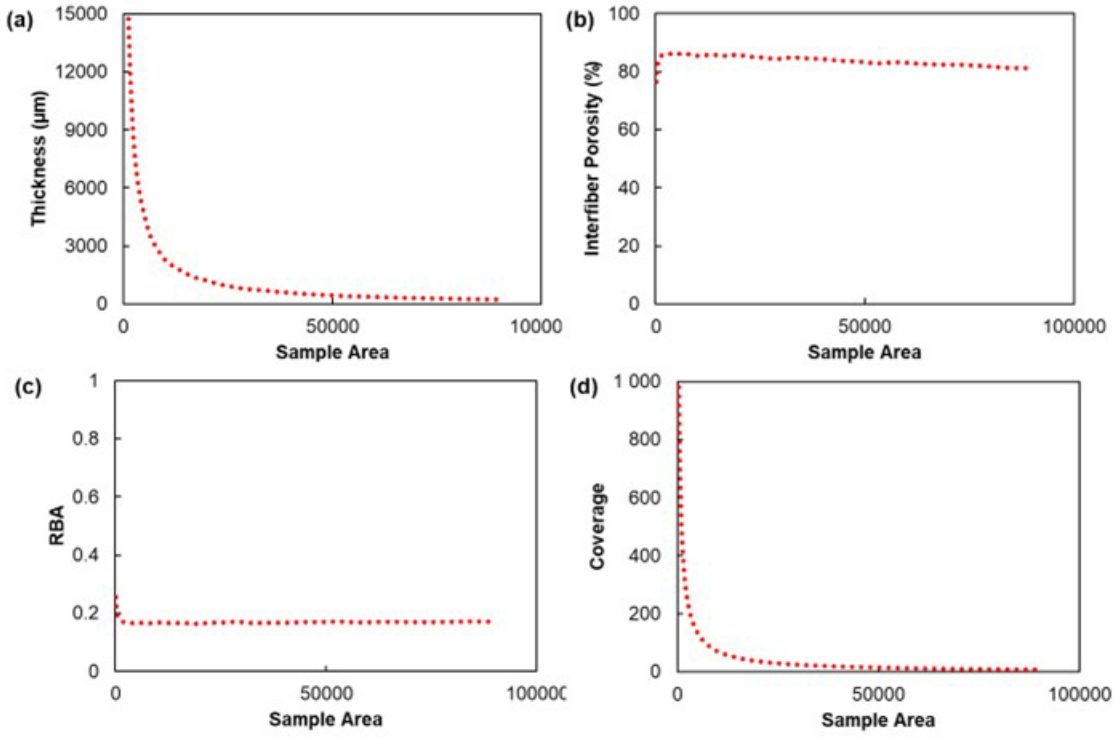

Fig. 8. Evolution of the (a) thickness, (b) interfiber porosity, (c) RBA, and (d) coverage of the XY plane for a eucalyptus structure

Validation of Computational Structures

To validate the predictive capacity of the structural properties of tissue structures, a comparison of the computational and experimental structures was performed. Figure 9 presents the beating influence on the paper thickness and porosity for computational simulated structures, validated with the experimental results presented in Fig. 6. Following our experimental results, a similar impact for the influence of computational structures was verified. Furthermore, the model proves to adjust to the experimental data. To relate simulations with experimental data, the fiber parameters needed to be defined. For the simulated structures, the EUC and EUC Slush pulps were defined as a fiber population that was the combination of four fiber models proposed by us in a previous publication (Morais *et al.* 2020b). Beating levels are implemented in the 3D model through the influence of fiber flexibility and collapse. It was evident that different fiber collapse degrees influenced the structural properties. For each beating level, different fiber wall thickness and lumen dimensions were tested, and structural properties were determined. The simulated computational structures were obtained for a fixed basis weight of 20, 40, and 60 g/m^2, identical to the experimental data.

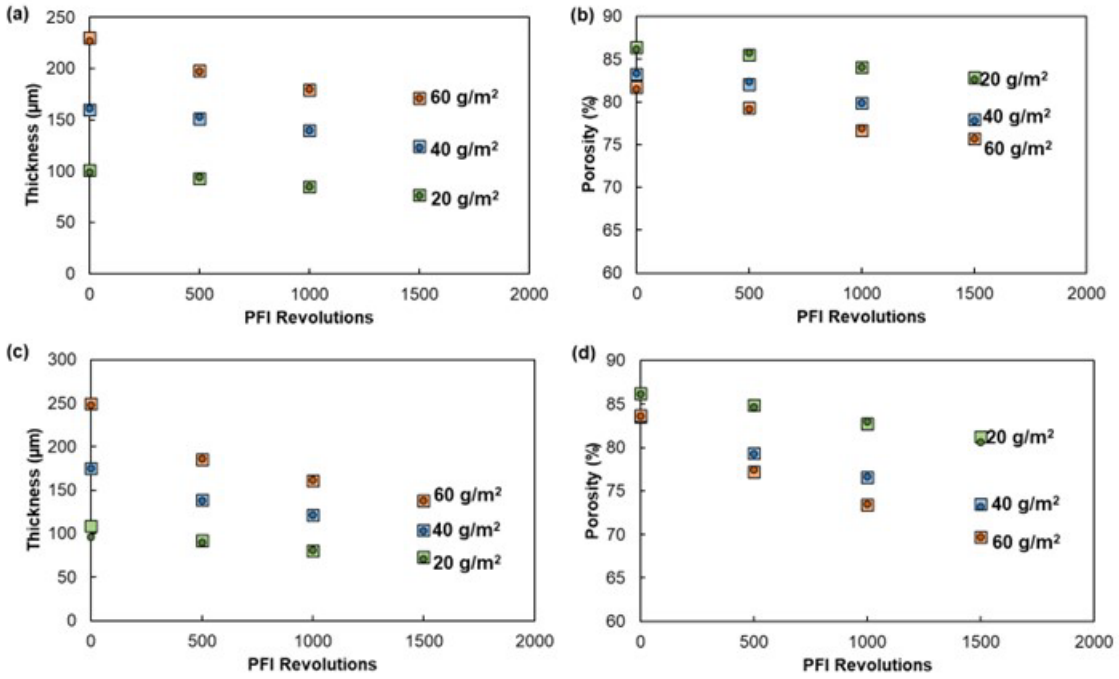

Fig. 9. Comparison of computational and experimental (a, c) thickness and (b, d) porosity as a function of PFI revolutions of (a, b) EUC and (c, d) EUC Slush handsheets with 20, 40, and 60 g/m^2. The computational results are presented with a circle symbol and the experimental results with a square symbol.

This entire process makes it possible to model the structures in 3D and predict the structural properties of a material with low basis weight and high porosity as in the case of tissue papers. Posteriorly, this strategy allows optimizing the various tissue materials, defining different furnish tissue scenarios. This is possible with the combination of an approach presented in the authors' previous publications (Morais *et al.* 2021a,b,c), in which mathematical models of multiple linear regression, artificial neural networks, robust linear regressions, and interpolation and extrapolation methods were used. These proposed

mathematical models consider the fiber morphological, suspension, and structural properties to forecast functional tissue properties (Morais and Curto 2022). Using these computational simulation methods, different fiber mixing and modification process strategies were evaluated considering the desired softness, strength, and absorption properties, including maximizing the eucalyptus pulp incorporation, with additives such as micro/nanofibrillated cellulose and biopolymer, and different eucalyptus pulps (Morais *et al.* 2021c). The results of the 3D fiber modeling, using the *voxelfiber*, were used to investigate the influence of fibers on the structural properties due to the good estimative of the simulated results with the experimental ones. Therefore, the bulk and porosity values predicted by the simulator, which are directly related to the paper thickness, are used in the models developed by the authors to predict the tissue functional properties, resulting in higher speed and flexibility of response, without the need to produce extensive laboratory structures (Morais and Curto 2022).

CONCLUSIONS

1. The purpose of this article was to present a computational approach to model fibers and tissue structures using a 3D fibrous material simulator, predicting their structural properties. These simulations were based on an initial experimental characterization of beaten and unbeaten eucalyptus fiber pulps, implementing these datasets in the model in order to benefit from modeling strategies considering the structural hierarchy at the fiber and structure level. The samples to build this model (Morais *et al.* 2020a) were independent of the samples to test the model. The 3D model includes key papermaking fiber properties and process operations, with a detailed fiber model. The model has shown good forecast capability for structural properties like paper thickness and porosity. It was found that this simulation studies approach constitutes a valuable tool to distinguish the influence of fiber characteristics like fiber flexibility and collapse on the structure densification, for example, that occurs with beating.
2. The computational results were validated with experimental structures produced in the laboratory, and the simulated results represented a good estimative of this real tissue paper network. The tissue structures were built by the random deposition of individually 3D fibers. The fibers were modeled using fiber dimensions and the structures made by them, according to image analysis methods. These parameters were changed independently, and the raw materials were defined as a fiber population with a combination of different fiber models, to allow the implementation of different degrees of fiber flexibility and collapse.
3. The possibility of modeling tissue materials, at the fiber level and 3D structure level, is crucial to predict the structural and functional properties and therefore optimize these types of products. The integration of the predicted and validated results of this 3D fiber-based simulator with the mathematical models built in the authors' recent work (Morais and Curto 2022), will make it possible to forecast and optimize the softness, strength, and absorption properties of tissue products. The combination of advanced computational tools and experimental design in the development of a simulator that mimics tissue products is an important milestone not only to support industrial production in furnish management and process optimization but also to design innovative tissue materials.

ACKNOWLEDGMENTS

This research was supported by Project InPaCTus – Innovative Products and Technologies from eucalyptus, Project Nº 21 874 funded by Portugal 2020 through European Regional Development Fund (ERDF) in the frame of COMPETE 2020 nº 246/AXIS II/2017.

The authors are very grateful for the support given by research unit Fiber Materials and Environmental Technologies (FibEnTech-UBI), on the extent of the project reference UIDB/00195/2020, funded by the Fundação para a Ciência e a Tecnologia, IP/MCTES through national funds (PIDDAC).

REFERENCES CITED

Alava, M. and Niskanen, K. (2006). "The physics of paper," *Rep. Prog. Phys.* 69(3), 669-723. DOI: 10.1088/0034-4885/69/3/R03

Bloch, J. -F. and Roscoat S. R. (2009). "Three-dimensional structural analysis," in: *Proc. Advances in Pulp and Paper Research, 14th Fundamental Research Symposium*, S. J. I'Anson (ed.), Oxford, UK, pp 599–664. DOI: 10.15376/frc.2009.2.599

Bloch, J. -F., Engin, M., and Sampson, W. W. (2019). "Grammage dependence of paper thickness," *Appita J*. 72(1), 30-40.

Chinga-Carrasco, G. and Helle, T. (2002). "Structure characterisation of pigment coating layer on paper by scanning electron microscopy and image analysis," *Nord. Pulp Pap. Res. J*. 17(3), 307-312. DOI: 10.3183/NPPRJ-2002-17-03-p307-312

Chinga-Carrasco, G. (2009). "Exploring the multi-scale structure of printing paper – A review of modern technology," *J. Microsc*. 234(3), 211-242. DOI: 10.1111/j.1365-2818.2009.03164.x

Conceição, E. L. T., Curto, J. M. R., Simões, R. M. S., and Portugal, A. T. G. (2010). "Coding a simulation model of the 3D structure of paper," in: *Computational Modeling of Objects Represented in Images*, R. P. Barneva, V. E. Brimkov, H. A. Hauptman, R. M. Natal Jorge, and J. M. R. S. Tavares (eds.), Springer, Berlin, pp. 299-310. DOI: 10.1007/978-3-642-12712-0_27

Curto, J. M. R., Conceição, E. L. T., Portugal, A. T. G., and Simões, R. M. S. (2011). "Three dimensional modeling of fibrous materials and experimental validation," *Materwiss*. *Werksttech*. 42(5), 370–374. DOI: 10.1002/mawe.201100790

Curto, J. M. R. (2012). *3D Computational Simulation and Experimental Characterization of Polymeric Stochastic Network Materials: Case Studies in Reinforced Eucalyptus Office Paper and Nanofibrous Materials*, Doctoral Thesis, Universidade da Beira Interior, Covilhã, Portugal.

de Assis, T., Reisinger, L. W., Pal, L., Pawlak, J., Jameel, H., and Gonzalez, R. W. (2018). "Understanding the effect of machine technology and cellulosic fibers on tissue properties – A review," *BioResources* 13(2), 4593-4629. DOI: 10.15376/biores.13.2.DeAssis

Dirrenberger, J., Forest, S., and Jeulin, D. (2014). "Towards gigantic RVE sizes for 3D stochastic fibrous networks," *Int. J. Solids Struct.* 51(2), 359–376. DOI: 10.1016/j.ijsolstr.2013.10.011

Dodson, C. T., Oba, Y., and Sampson, W. W. (2001). "On the distributions of mass, thickness and density in paper," *Appita J.* 54(4), 385-389.

Dodson, C. T. J., Handley, A. G., Oba, Y., and Sampson, W. W. (2002). "The pore radius distribution in paper. Part I: The effect of formation and grammage," *Appita J.* 56(4), 275-280. DOI: 10.1007/s001840200212

Doškář, M., Zeman, J., Jarušková, D., and Nová, J. (2018). "Wang tiling aided statistical determination of the representative volume element size of random heterogeneous materials," *Eur. J. Mech. A/Solids* 70, 280-295. DOI: 10.1016/j.euromechsol.2017.12.002

du Roscoat, S. R., Decain, M., Thibault, X., Geindreau, C., and Bloch, J. -F. (2007). "Estimation of microstructural properties from synchrotron X-ray microtomography and determination of the REV in paper materials," *Acta Mater.* 55(8), 2841-2850. DOI: 10.1016/j.actamat.2006.11.050

Giacomozzi, D. E., and Joutsimo, O. (2015). "Drying temperature and hornification of industrial never-dried *Pinus radiata* pulps. 1. Strength, optical, and water holding properties," *BioResources* 10(3), 5791-5808. DOI: 10.15376/biores.10.3.5791-5808

Giacomozzi, D. E., and Joutsimo, O. (2017). "Drying temperature and hornification of industrial never-dried *Pinus radiata* pulps. 2. Voith Sulzer refining," *BioResources* 12(1), 1532-1547. DOI: 10.15376/biores.12.1.1532-1547

Grothaus, M., Klar, A., Maringer, J., Stilgenbauer, P., and Wegener, R. (2014). "Application of a three-dimensional fiber lay-down model to non-woven production processes," *J. Math. Industry* 4, 4. DOI: 10.1186/2190-5983-4-4

Hotaling, N. A., Bharti, K., Kriel, H., and Simon, C. G. (2015). "DiameterJ: A validated open source nanofiber diameter measurement tool," *Biomaterials* 61, 327-338. DOI: 10.1016/j.biomaterials.2015.05.015

Hu, A., Li, X., Ajdari, A., Jiang, B., Burkhart, C., Chen, W., and Brinson, L. C. (2018). "Computational analysis of particle reinforced viscoelastic polymer nanocomposites – Statistical study of representative volume element," *J. Mech. Phys. Solids* 114, 55-74. DOI: 10.1016/j.jmps.2018.02.013

Jirsák, O., Henyš, P., and Pokorný, P. (2022). "The simulation of mechanical responses of nonwoven fabrics using an improved meshless discrete algorithm," *J. Text. Inst.* DOI: 10.1080/00405000.2022.2052451

Joutsimo, O. P., and Asikainen, S. (2013). "Effect of fiber wall pore structure on pulp sheet density of softwood kraft pulp fibers," *BioResources* 8(2), 2719-2737. DOI: 10.15376/biores.8.2.2719-2737

Kallmes, O. J. and Bernier, G. A. (1963). "Estimating the thickness of pulped wood fibres," *Nature* 197, 1330. DOI: 10.1038/1971330a0

Kanit, T., Forest, S., Galliet, I., Mounoury, V., and Jeulin, D. (2003). "Determination of the size of the representative volume element for random composites: Statistical and numerical approach," *Int. J. Solids Struct.* 40(13-14), 3647-3679. DOI: 10.1016/S0020-7683(03)00143-4

Kettil, G., Målqvist, A., Mark, A., Edelvik, F., Fredlund, M., and Wester, K. (2018). "A multiscale methodology for simulation of mechanical properties of paper," in: *Proc. at 6th European Conference on Computational Mechanics (ECCM 6) and 7th Eur. Conference on Computational Fluid Dynamics (ECFD 7)*, Glasgow, UK, pp. 1115.

Lavrykov, S., Lindström, S. B., Singh, K. M., and Ramarao, B. V. (2012). "3D network simulations of paper structure," *Nord. Pulp Paper Res. J.* 27(2), 256-263. DOI: 10.3183/NPPRJ-2012-27-02-p256-263

Lawrence, M. and Jiang, Y. (2017). "Porosity, pore size distribution, micro-structure," in: *Bio-aggregates Based Building Materials*, S. Amziane and F. Collet (eds.), Springer,

Dordrecht, pp. 39-70. DOI: 10.1007/978-94-024-1031-0_2

Martins, V. D. F., Cerqueira, M. A., Fuciños, P., Garrido-Maestu, A., Curto, J. M. R., and Pastrana, L. M. (2018). "Active bi-layer cellulose-based films: Development and characterization," *Cellulose* 25, 6361-6375. DOI: 10.1007/s10570-018-2021-y

Marulier, C., Dumont, P. J. J., Orgéas, L., du Roscoat, S. R., and Caillerie, D. (2015). "3D analysis of paper microstructures at the scale of fibres and bonds," *Cellulose* 22, 1517-1539. DOI: 10.1007/s10570-015-0610-6

Masrol, S. R., Ibrahim, M. H. I., Adnan, S., Tajudin, M. S. A. A., Raub, R. A., Razak, S. N. A. A., and Zain, S. N. F. M. (2017). "Effects of total chlorine free (TCF) bleaching on the characteristics of chemi mechanical (CMP) pulp and paper from Malaysian durian (*Durio zibethinus murr.*) rind," *Jurnal Teknologi* 79(4), 55-64. DOI: 10.11113/jt.v79.9803

Mirkhalaf, S. M., Pires, F. M. A., and Simões, R. (2016). "Determination of the size of the representative volume element (RVE) for the simulation of heterogeneous polymers at finite strains," *Finite Elem. Anal. Des.* 119, 30-44. DOI: 10.1016/j.finel.2016.05.004

Morais, F. P., Bértolo, R. A. C., Curto, J. M. R., Amaral, M. E. C. C., Carta, A. M. M. S., and Evtyugin, D. V. (2019). "Comparative characterization of eucalyptus fibers and softwood fibers for tissue papers applications," *Mater. Lett.: X* 4, 1000028. DOI: 10.1016/j.mlblux.2019.100028

Morais, F. P., Carta, A. M. M. S., Amaral, M. E., and Curto, J. M. R. (2020a). "Experimental 3D fibre data for tissue papers applications," *Data in Brief* 30, 105479. DOI: 10.1016/j.dib.2020.105479

Morais, F. P., Carta, A. M. M. S., Amaral, M. E., and Curto, J. M. R. (2020b). "3D fiber models to simulate and optimize tissue materials," *BioResources* 15(4), 8833-8848. DOI: 10.15376/biores.15.4.8833-8848

Morais, F. P., Simões, R. M. S., and Curto, J. M. R. (2020c). "Biopolymeric delivery systems for cosmetic applications using *Chlorella vulgaris* algae and tea tree essential oil," *Polymers* 12(11), 2689. DOI: 10.3390/polym12112689

Morais, F. P., Carta, A. M. M. S., Amaral, M. E., and Curto, J. M. R. (2021a). "Micro/nano-fibrillated cellulose (MFC/NFC) fibers as an additive to maximize eucalyptus fibers on tissue paper production," *Cellulose* 28, 6587-6605. DOI: 10.1007/s10570-021-03912-9

Morais, F. P., Carta, A. M. M. S., Amaral, M. E., and Curto, J. M. R. (2021b). "An innovative computational strategy to optimize different furnish compositions of tissue materials using micro/ nanofibrillated cellulose and biopolymer as additives," *Polymers* 13(15), 2397. DOI: 10.3390/polym13152397

Morais, F. P., Carta, A. M. M. S., Amaral, M. E., and Curto, J. M. R. (2021c). "Computational simulation tools to support the tissue paper furnish management: Case studies for the optimization of micro/nano cellulose fibers and polymer-based additives," *Polymers* 13(22), 3982. DOI: 10.3390/polym13223982

Morais, F. P., and Curto, J. M. R. (2022). "Challenges in computational materials modelling and simulation: A case-study to predict tissue paper properties," *Heliyon.* 8(5), e09356. DOI: 10.1016/j.heliyon.2022.e09356

Muneri, A. (1997). "Kraft pulping properties of *Acacia mearnsii* and *Eucalyptus grandis* grown in Zimbabwe," *South. Afr. For. J.* 179(1), 13-19. DOI: 10.1080/10295925.1997.9631148

Neumann, M., Staněk, J., Pecho, O. M., Holzer, L., Beneš, V., and Schmidt, V. (2016).

"Stochastic 3D modeling of complex three-phase microstructures in SOFC-electrodes with completely connected phases," *Comput. Mater. Sci.* 118, 353-364. DOI: 10.1016/j.commatsci.2016.03.013

Niskanen, K. J., Nilsen, N., Hellen, E., and Alava, M. J. (1997). "KCL-PAKKA: Simulation of the 3D structure of paper," in: *Proceedings of The Fundamentals of Papermaking Materials*, Cambridge, pp. 1273-1291. DOI: 10.15376/frc.1997.2.1273

Paavilainen, L. (1993a). "Conformability – flexibility and collapsibility – of sulphate pulp fibers," *Pap. Puu-Pap. Tim.* 5(9-10), 689-702.

Paavilainen, L. (1993b). "Importance of cross-dimensional fiber properties and coarseness for the characterization of softwood sulphate pulp," *Pap. Puu-Pap. Tim.* 75(5) 343-351.

Pourdeyhimi, B., Mazé, B., and Tafreshi, H. V. (2006). "Simulation and analysis of unbonded nonwoven fibrous structures," *J. Eng. Fibers Fabr.* 1(2), 47-65. DOI: 10.1177/155892500600100204

Pulkkinen, I., Ala-Kaila, K., and Aittamaa, J. (2006). "Characterization of wood fibers using fiber property distributions," *Chem. Eng. Process.* 45(7), 546-554. DOI: 10.1016/j.cep.2005.12.003

Raunio, J. -P. and Ritala, R. (2012). "Simulation of creping pattern in tissue paper," *Nord. Pulp Paper Res. J.* 27(2), 375-381. DOI: 10.3183/NPPRJ-2012-27-02-p375-381

Raunio, J. -P. and Ritala, R. (2013). "Method for detecting free fiber ends in tissue paper," *Meas. Sci. Technol.* 24(12), 125206. DOI: 10.1088/0957-0233/24/12/125206

Raunio, J. -P., Löyttyniemi, T., and Ritala, R. (2018). "Online quality evaluation of tissue paper structure on new generation tissue machines," *Nord. Pulp Paper Res. J.* 33(1), 133-141. DOI: 10.1515/npprj-2018-3004

Rowland, S. P. (1977). "Cellulose: Pores, internal surfaces, and water interface," in: *Textile and Paper Chemistry and Technology,* J. C. Arthur (ed.), American Chemical Society, Washington, DC, pp. 20-45.

Sampson, W. W. (2009). "Materials properties of paper as influenced by its fibrous architecture," *Int. Mater. Rev.* 54(3), 134-156. DOI: 10.1179/174328009X411154

Seth, R. S. (2001). "The difference between never-dried and dried chemical pulps," *Solutions! (Norcross, Ga)* 1(1), 1-23.

Sun, J., Yan, K., Zhu, Y., and Hong, J. (2021). "A high-similarity modeling method for low-porosity porous material and its application in bearing cage self-lubrication simulation," *Materials* 14(18), 5449. DOI: 10.3390/ma14185449

Tourtollet, G. E. P., Cottin, F., Cochaux, A., and Petit-Conil, M. (2003). "The use of MorFi analyser to characterize mechanical pulps," in: *Proceedings of the International Mechanical Pulping Conference*, Quebec City, Canada, pp. 225-232.

Wiltsche, M., Donoser, M., Kritzinger, J., and Bauer, W. (2011). "Automated serial sectioning applied to 3D paper structure analysis," *J. Microsc.* 242(2), 197-205. DOI: 10.1111/j.1365-2818.2010.03459.x

Xie, J., Fang, J., Chen, L., Jiao, W., Yang, Z., and Chen, L. (2022). "Micro-scale modeling of 3D needled nonwoven fiber preforms," *Comps. Struct.* 281, article no. 114995. DOI: 10.1016/j.compstruct.2021.114995

Article submitted: January 6, 2022; Peer review completed: April 25, 2022; Revised version received and accepted: May 20, 2022; Published: May 23, 2022.
DOI: 10.15376/biores.17.3.4206-4225